

EVALUATION OF PROCESS PARAMETERS ON SURFACE ROUGHNESS AND RESIDUAL STRESSES IN HIGH-SPEED END MILLING OF Al-Si-Mg-Fe ALLOY

S. MADHAVA REDDY AND A. CHENNAKESAVA REDDY

ABSTRACT: *This paper presents a study of the Taguchi design application to surface quality in a CNC end milling operation. In the present investigation, the straight flute end-milling cutter was used for machining of Al-Si-Mg-Fe alloy work pieces. The surface roughness depends upon the cutting speed, feed rate and depth of cuts. The influence of high-speed end milling on surface roughness and residual stresses in Al-Si-Mg-Fe alloy work pieces, which were cast by the sand, investment and die casting method, was investigated. The results concluded that the surface roughness decreases with increase in the cutting speed, increases with increase in feed rate and increases with increase in depth of cut. The residual induced in the work piece increases with increase in feed rate and increases with increase in depth of cut. The T6 heat treatment for Al-Si-Mg-Fe alloy offers a low average residual stress during the high-speed milling operation.*

Key words: *Taguchi design, surface roughness, residual stresses, milling operations*

1. INTRODUCTION

Under periodically varying milling forces, the cutting tool experiences both static and dynamic deformations, which are passed as dimensional, and surface finish errors to the product. The conditions that affect the surface finish are feed, speed, material, and tool geometry. The residual stresses may be induced during machining due to milling forces and heat generation.

High-speed machining is a relative term from a materials perspective, since different materials are machined with different cutting speeds to insure adequate tool life. The cutting speed determines whether a material would form continuous or segmented chips. The high-speed machining is defined quantitatively in terms of cutting speed ranges [1]:

- High-speed machining (600 to 1800 m/min)
- Very high-speed machining (1800 to 18000 m/min)
- Ultra high-speed machining (18000 m/min) and above.

The high-speed machining is used in the defense, aerospace and automobile industries. Most aerospace manufacturers have implemented high-speed machining in end milling using small-size cutters. The most common work material was aluminum; there was no tool wear limitation, particularly when carbide cutters were used [1]. Also, in the aerospace industry, the major application of high-speed machining has been in thin walled structures.

In the present work, the influence of high-speed end milling on surface roughness and residual stresses in Al-Si-Mg-Fe alloy work pieces, which were cast by the sand, investment and die casting method, was investigated. The end mills have cutting teeth on the end as well as on the periphery of the cutter. In the present investigation, the straight flute end-milling cutter was used for machining of Al-Si-Mg-Fe alloy work pieces.

The effects of high speed milling of cast Al-Si-Mg-Fe alloys were investigated in terms of surface morphology and residual stresses of work piece. The surface morphology was investigated through the measurement of surface roughness and scanning electron microscopy (SEM). The residual stresses were evaluated by the X-ray measurements

2. DESIGN OF EXPERIMENTS

The Al-Si-Mg-Fe alloy was prepared and chemical analysis of their ingredients was done. The chemical composition of alloy is given in Table 1. The sand mould, investment shell, and cast iron mould were employed to prepare the samples for high-speed end milling.

Table 1
Chemical Composition of Alloys

<i>Alloy</i>	<i>Composition determined spectrographically, %</i>						
<i>Element</i>	<i>Al</i>	<i>Si</i>	<i>Mg</i>	<i>Fe</i>	<i>Cu</i>	<i>Mn</i>	<i>Cr</i>
<i>%</i>	85.22	9.0	2.0	3.5	0.01	0.25	0.02

Straight flute end milling cutters are generally used for milling either soft or tough materials. In order to develop monitoring functions, displacement sensors are installed on the spindle unit of a high precision machining center. The machine used in the study is a vertical type-machining center (figure 1).

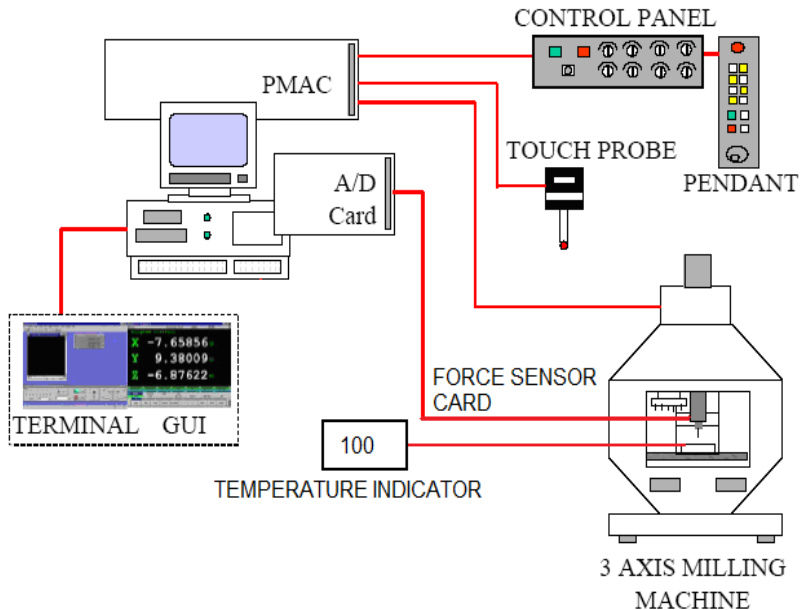


Figure1: High Speed Vertical Milling Center

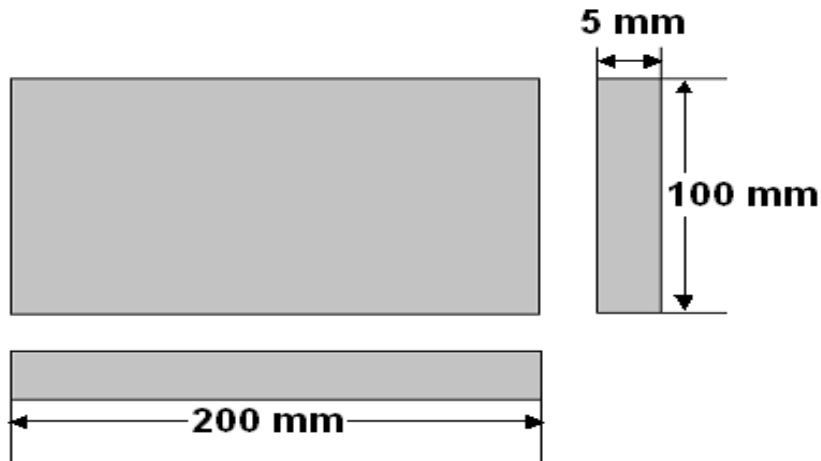


Figure 2: The Dimensions of Workpiece used High-Speed Milling

The PCD end-milling cutter having four straight flutes was used in this investigation. High-pressure coolant jet was employed for cooling and lubrication of the high-speed machining operations. The spindle has constant position preloaded bearings with oil-air lubrication, and the maximum rotational speed is 20 000 rpm. The dimensions of the workpiece used in the high-speed milling are shown in figure 2.. The temperature of the workpiece material was measured using thermocouple.

2.1 Selection of the quality characteristics

The selection of quality characteristics to measure as experimental outputs greatly influences the number of tests that will have to be done statistically meaningful. The quality characteristics, which were selected to influence the high-speed end milling of Al-Si-Mg-Fe alloy, are the surface roughness and residual stresses.

2.2 Selection of machining parameters

This is the most important phase of investigation. If important parameters are unknowingly left out of the experiment, then the information gained from the experiment will not be in a positive sense. The parameters, which influence the performance of the high-speed end milling, are:

- Microstructure of Al-Si-Mg-Fe alloy
- Cutting speed
- Feed rate
- Depth of cut
- Coolant

Since the high-speed milling involves high cost of machining, the process parameters were optimized using Taguchi's method [2]. Taguchi techniques offer potential savings in test time and money by more efficient testing strategies. Not only are savings in test time and cost available but also a more fully developed product or process will emerge with the use of better experimental strategies.

Table 2
Control Parameters and Levels

Parameter	Symbol	Level – 1	Level – 2	Level-3
Casting	c	Sand casting	Investment casting	Die casting
Cutting speed, m/min	n	600	1200	1800
Feed rate, mm/min	f	1000	3000	5000
Depth of cut, mm	d	0.2	0.4	0.6

Control parameters are those parameters that a manufacturer can control the design of high-speed end milling. The levels chosen for the control parameters were in the operational range of the high-speed end milling. Trial runs were conducted by choosing one of the machining parameters and keeping the rest of them at constant values. The selected levels for the chosen control parameters are summarized in Table – 2. Each of the four control parameters was studied at three levels.

2.4 Assignment of control parameters

The orthogonal array, L_9 was selected for the high-speed end milling. The parameters were assigned to the various columns of orthogonal array (OA). The assignment of parameters along with the OA matrix is given in Table–3.

Table 3
Orthogonal Array (L_9) and Control Parameters

Treat No.	n	f	d	c
1	1	1	1	1
2	1	2	2	2
3	1	3	3	3
4	2	1	2	3
5	2	2	3	1
6	2	3	1	2
7	3	1	3	2
8	3	2	1	3
9	3	3	2	1

2.5 Preparation of Al-Si-Mg-Fe alloy melts

An Al-Si alloy was melted in an oil-fired furnace. During melting pure aluminum, pure magnesium in the solid form and pure iron in the liquid form were added to the liquid melt according to the charge calculation. The melting losses of aluminum and magnesium were taken into account while preparing the charge. During melting the charge was fluxed with coveral-11 (a Foseco company product) to prevent dressing. The molten metal was then degasified by tetrachlorethane (in solid form) using a plunger ending in a small inverted crucible. The melt was also modified with sodium in the crucible before pouring. The crucibles were made of graphite [3-6]. The dross removed melt was finally gravity poured into the preheated sand, investment and die (iron) cast moulds. The solidified cast samples were solution treated under the T6 conditions.

2.6 Optical microscopy and scanning electron microscopy (SEM)

The optical microscopy was used to determine the grain size and shape and distribution of various phases and inclusions, which could affect the mechanical properties of the castings. The specimens to be observed under an optical microscope were prepared using standard procedures. The surfaces of the high-speed machined test samples were examined in scanning electron microscope (SEM) to determine the surface morphology. The samples for SEM observation were obtained from the machined specimens by sectioning parallel to the machined surface and the scanning was carried in IICT, S-3000N Toshiba.

2.7 Hole –Drilling strain gauge

The most widely used practical technique for measuring residual stresses is the hole-drilling strain gauge method described in ASTM Standard E837. With this method, a specially configured electrical resistance strain gauge rosette was bonded to the surface of the test object and a small shallow hole was drilled through the center of the rosette. The drilled hole is typically 2.0 mm both in diameter and depth. The local changes in strain due to introduction of the hole were measured and the relaxed residual stresses were computed from these measurements.

2.8 Techniques to analysis results

After all tests were conducted, the decisions were made with the assistance of the following analytical techniques:

- **Analysis of variance:** ANOVA is a statistically based, objective decision-making tool for detecting any differences in average performance of groups of items tested. The decision takes variation into account. The parameter which has Fisher's ratio (F-ratio) larger than the criterion (F-ratio from the tables) are believed to influence the average value for the population, and parameters which has an F-ratio less than the criterion are believed to have no effect on the average. Percent contribution indicates the relative power of a parameter to reduce variation.
- **Plotting method:** To plot the effect of influential factors, the average result for each level must be calculated first. The sum of the data associated with each level in the OA column divided by the number of tests for that level would provide the appropriate averages. Plots may be made with equal increments between levels on the horizontal axes of the graphs to show the relative strengths of the factors. The strength of a factor is directly proportional to the slope of the graph.
- **Confirmation tests:** The key task was the determination of the preferred combination of the levels of the parameters indicated to be significant by the analytical methods. The insignificant parameters may be set at any desirable levels. The purpose of the confirmation test was to validate the conclusions drawn during the analysis phase.

3. RESULTS

The experiments were conducted randomly and repeated twice.

3.1 Effect of process variables on the surface roughness

The surface roughness (R_a) values under various combinations of machining variables are given in Table 4. The roughness profiles of various machining conditions are shown in Figures 1 – 6. The summary of ANOVA (analysis of variance) for surface roughness is shown in Table 5. According to the analysis of variance, all the process variables have significant influence on the variation of surface roughness. The percent contribution indicates that the variable d (depth of cut) all by itself contributes the most toward the variation observed in the surface roughness (R_a values): almost 73.45%. The variable f (feed rate) contributes over 13.42% of the total variation observed. The variables n (cutting speed) and c (type of casting) contribute 7.02% and 6.09% respectively to the total variation in surface roughness.

Table 4
Experimental Results of Surface Roughness

Treat No.	Surface roughness (R_a), microns	
	Trial-1	Trial-2
1	3.76	3.72
2	4.48	4.34
3	5.52	5.56
4	3.69	3.75
5	5.19	5.24
6	3.82	3.91
7	4.56	4.67
8	3.04	2.89
9	4.68	4.61

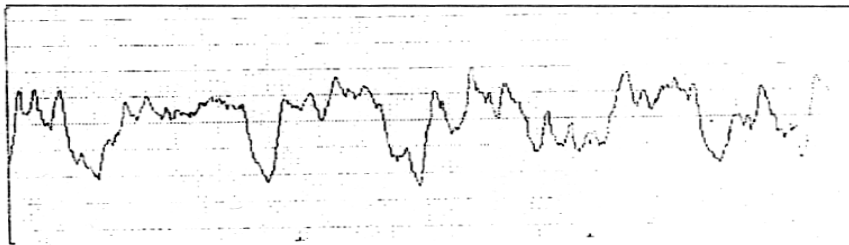


Figure 3: Treatment No:1; $R_a = 3.76$ microns

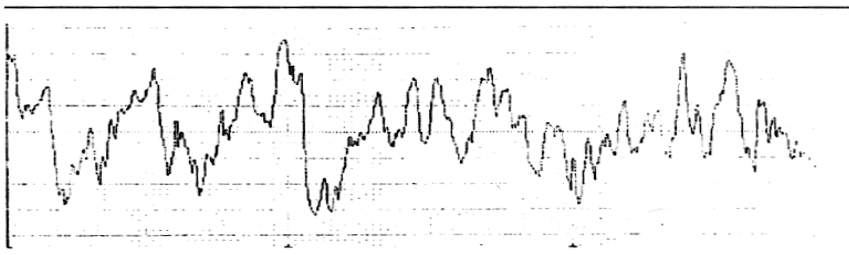


Figure 4: Treatment No:3; $R_a = 5.52$ microns

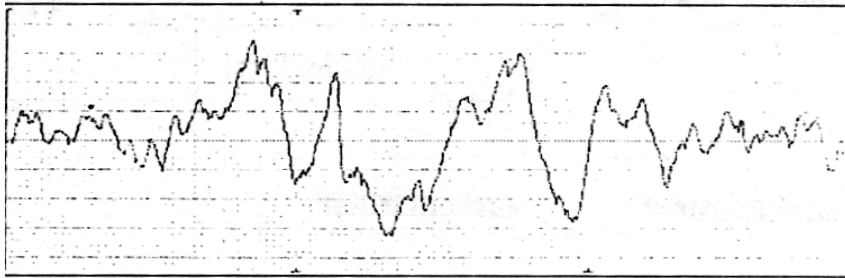


Figure 5: Treatment No:5; Ra = 5.19 microns

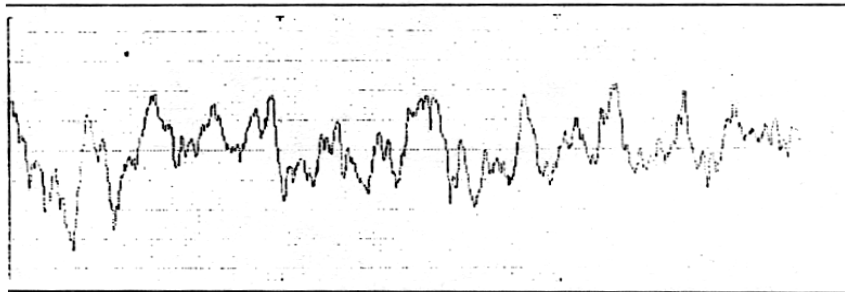


Figure 6: Treatment No:6; Ra = 3.82 microns

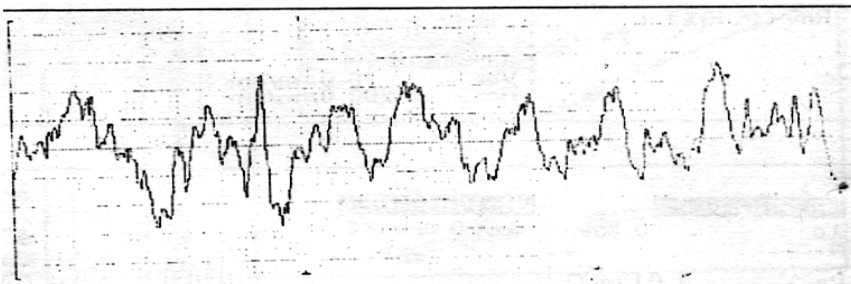


Figure7: Treatment No:7; Ra = 4.56 microns

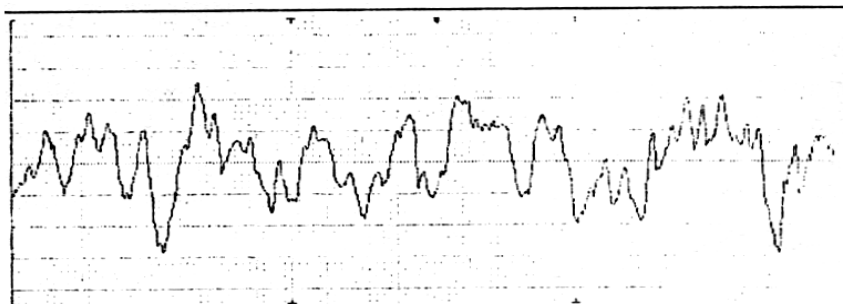


Figure 8: Treatment No:9; Ra = 4.68 microns

Table 5
ANOVA Summary of Surface Roughness

Column No	Source	Sum 1	Sum 2	Sum 3	SS	v	V	F	P
1	n	124.944	109.227	99.634	0.726433	2	0.36322	85.4628	7.02
2	f	97.204	105.672	131.602	1.399433	2	0.69972	164.639	13.42
3	d	74.483	108.800	157.491	7.6969	2	3.8485	905.518	73.45
4	c	123.307	110.768	99.634	0.630433	2	0.31522	74.1686	6.09
5	e	----	----	---	0.03825	9	0.00425	-----	-----
6	T	----	----	----	10.49145	17	-----	-----	-----

The effect of cutting speed on the surface roughness is shown in Figure 9. The surface roughness decreases with increase in the cutting speed. Indeed, low speeds are used for rough cutting and high speeds are employed for fine finishing in the machine shop.

The effect of feed rate on the surface roughness is illustrated in Figure 10. It can be understood that the surface roughness increases with increase in feed rate. The cutting with a tool having a certain wear generates surface roughness than a fresh tool, because the tool wear is proportional to the cutting feed rate and roughness is a reproduction of the tool nose profile on the workpiece surface.

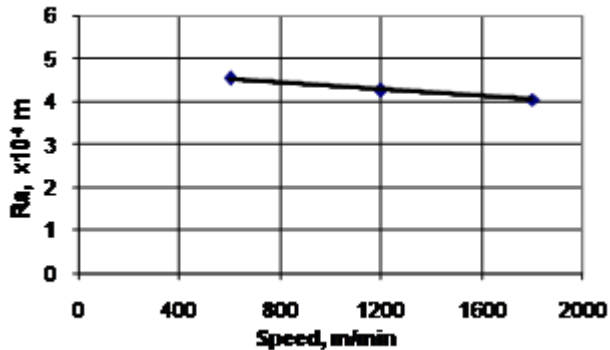


Figure 9: Effect of Cutting Speed on the Surface Roughness

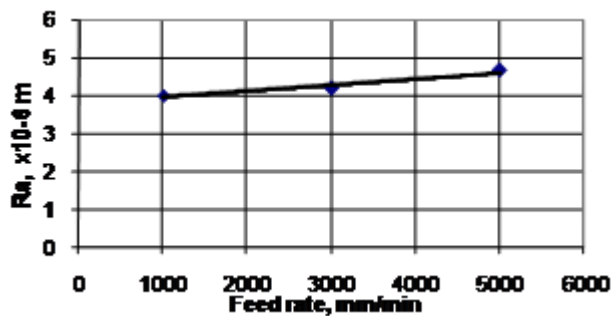


Figure 10: Effect of Feed Rate on the Surface Roughness.

The variation of surface roughness of the workpiece on account of depth of cut is shown in Figure 11. It is clearly seen that the roughness increases with increase in depth of cut. Depth of cut plays major role on the roughness of the workpiece surface. The rigidity of the cutting and machine is largely depending upon the depth of cut. The rigidity decreases with increase in depth of cut [7]. The amount of heat generation increases with increase in depth of cut, because the cutting tool has to remove large volume of material from the workpiece. The plastic deformation of the workpiece is proportional to the amount of heat generation in the workpiece. Large amount of plastic deformation in the workpiece promotes roughness on the workpiece surface.

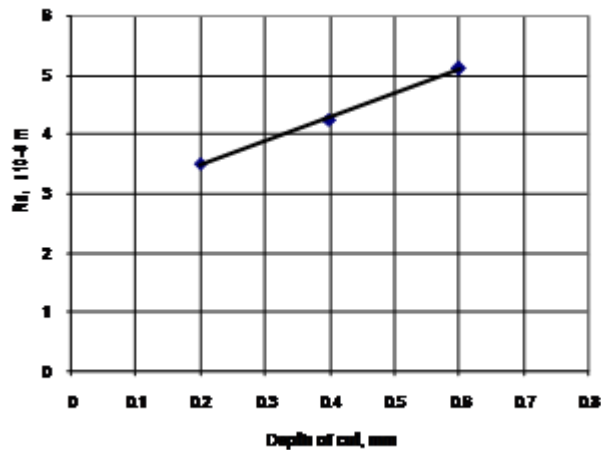


Figure 11: Effect of Depth of Cut on the Surface Roughness.

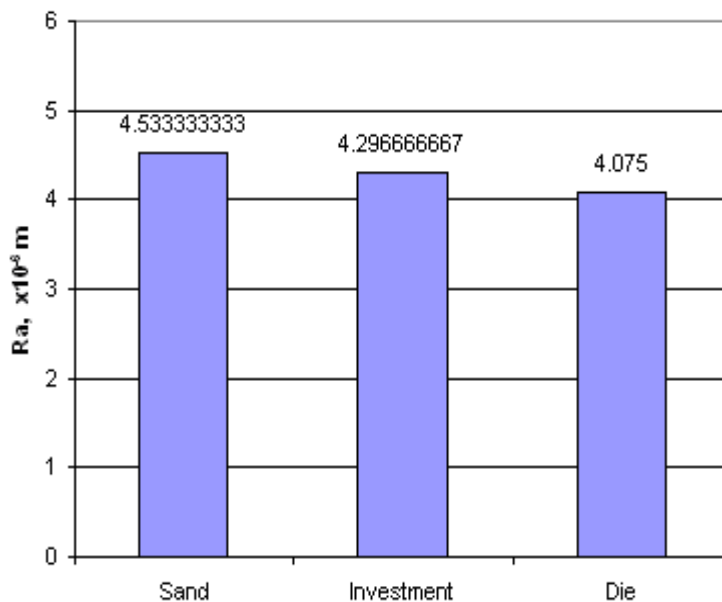


Figure 12. Effect of Casting Condition on the Surface Roughness.

The variation of surface roughness with casting condition is shown in Figure 12. The sand cast specimens promote greater roughness than die cast specimens. This is due to fact that the sand specimens have coarse grain structure, whereas the die cast specimens have fine grain structure. The surface roughness of investment cast specimens is intermediate to the sand and die cast specimens.

4. Effect of process variables on the residual stresses

The residual stresses were measured in two (x- and y-) directions on the workpiece surface:

- X-milling direction on the workpiece surface aligned with workpiece longitudinal axis.
- Y-direction on the workpiece surface perpendicular to x-axis. It is assumed that the stress in the direction perpendicular to the milled surface is negligible.

Table 6
Experimental Results of Residual Stress

Treat No.	Stress, N	
	x-direction	y-direction
1	-54	-51
2	0.5	1
3	14	15
4	2	1.5
5	8	7
6	-32	-35
7	5.5	5
8	-26	-28
9	6	5.5

The measured stresses are tabulated in Table 6. The ANOVA summary of residual stress is given in Table-6. According to the analysis of variance, depth of cut and feed rate have significant influence on the variation of residual stress. The percent contribution indicates that the variable d (depth of cut) all by itself (90.26%) contributes the most toward the variation observed in the residual stress. The variable f (feed rate) contributes over 4.67% of the total variation observed. The variables n (cutting speed) and c (type of casting) have negligible effect the total variation in residual stress.

Table 6
ANOVA Summary of Residual Stress

Source	Sum 1	Sum 2	Sum 3	SS	v	V	F	P
n	925.04	392.04	170.67	153.03	2	76.51	55.09	1.82
f	1380.17	234.38	117.04	396.86	2	198.43	142.87	4.67
d	8512.67	45.38	495.04	7718.36	2	3859.18	2778.61	90.26
c	1027.04	504.17	77.04	273.53	2	136.76	98.47	3.23
e	----	----	---	12.5	9	1.39	-----	----
T	----	----	----	8554.27	17	-----	-----	----

The effect of feed rate on the residual stress induced in the workpiece is shown in Figure 13. The residual induced in the workpiece increases with increase in feed rate. The surface residual stresses in the milling direction x- and in the orthogonal direction y- detected for every milling condition are always compressive. The influence of depth of cut is severe on the induction of residual stresses in the workpiece (Figure 14). The induced residual stresses during milling can be attributed mainly to two reasons:

- The spreading of material (plastic deformation) by the cutting tool leads to residual compressive stresses.
- The thermal heating due to the friction between workpiece surface and tool, which leads to tensile residual stresses.

For working condition with a higher material removal rate probably the thermal effect is more important than the spreading of material.

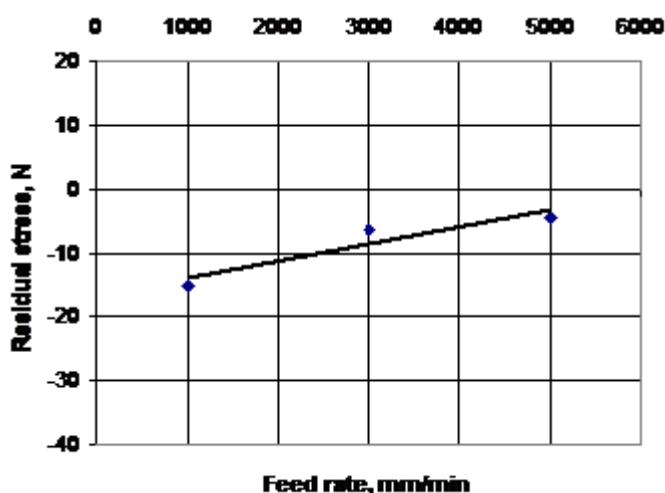


Figure 13. Effect of feed rate on the residual stress

In the SEM micrography (Figure15(a)), the white lines parallel to the milling direction are caused by the tearing of material. The tearing of material is observed with deeper depth of cuts. In Figure15(b) the white lines caused by tearing are less evident and the spreading of material is observed. The spreading of material is resulted with lower depth of cuts.

5. Discussions

The geometrical irregularities in the material machined by chip removal processes can be classified into four categories as follows:

1. **First order:** The irregularities caused by inaccuracies present in the machine tool
 - Irregularities caused due to lack of straightness of guide ways on which the tool moves.
 - Irregularities resulted due to deformation of work under the action of cutting forces
2. **Second order:** The irregularities caused due to vibrations of any kind
 - Chatter marks on the surface

3. **Third order:** The irregularities caused due to feed, depth of cut and speed
 - Feed mark of the cutting tool
4. **Fourth order:** The irregularities resulted due to the rupture of material during the separation of the chip.

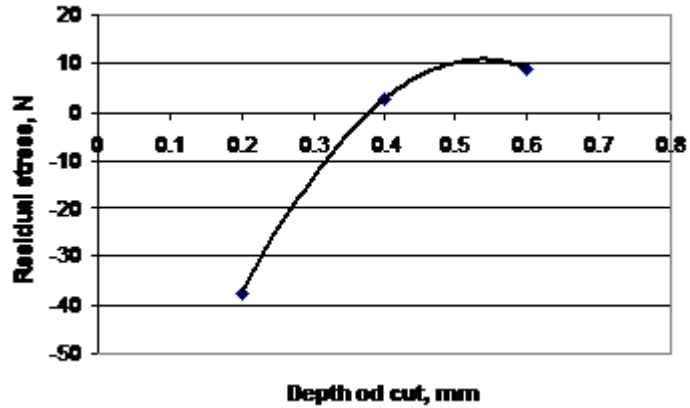


Figure 14: Effect of depth of cut on the residual stress

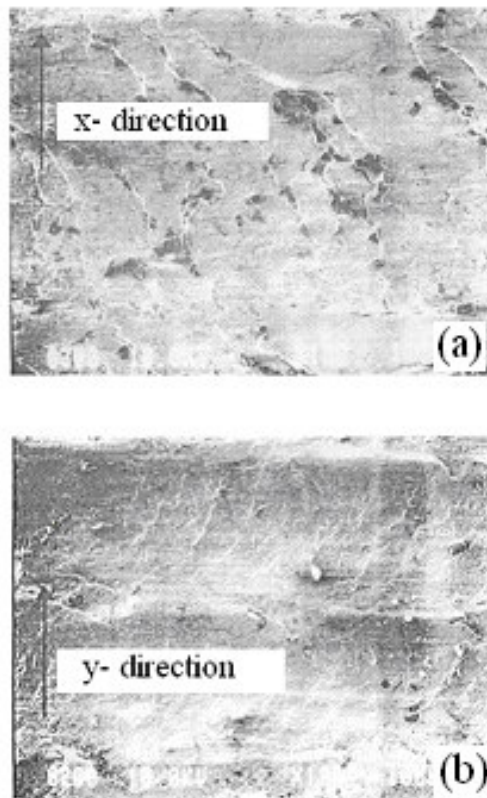


Figure 15: Surface morphology after high-speed milling (SEM)

In the present work, the first order geometrical irregularities were not observed. The second order geometrical irregularities were also not witnessed due to vibrations during machining, because the high-speed machining center was purchased one year back only. The third order geometric irregularities were noticed due the influence of cutting parameters such as cutting speed, depth of cut and feed rate. Figure 13 indicates the feed marks of the cutting tool. The fourth order geometrical irregularities were also observed due to tearing of the Al-Si-Mg-Fe alloy workpieces (figure 13). The tearing is the result of deeper depth of cuts.

The T6 heat treatment for Al-Si-Mg-Fe alloy offers a low average residual stress during the high-speed milling operation. The presence of aluminum dendrites, primary silicon, eutectic phase and intermetallic compounds might be attributed to the improvement of surface finish on high-speed machining of the Al-Si-Mg-Fe alloy work pieces.

5. Conclusions

The surface roughness depends upon the cutting speed, depth of cuts and feed rates. The surface roughness decreases with an increase in the cutting speed and , increases with increase in feed rate and depth of cut. The residual stress induced in the work piece increases with increase in feed rate and depth of cut. This behaviour can be attributed to the tearing of material is observed with deeper depth of cuts. The white lines caused by tearing are less evident and the spreading of material is observed. The spreading of material is resulted with lower depth of cuts.

References

- [1] Tedward T., Aluminium casting alloys and properties, *Modern Castings*, 840-849, 1965
- [2] Chennakesava Reddy A., and Shamraj V.M., Reduction of cracks in the cylinder liners choosing right process variables by Taguchi method, *Foundry*, 10(4), 47-50, 1998.
- [3] Iyer A. and Sadhu P.N., Metal treatment practices in aluminum die casting industry, *Indian Foundry Journal*, 45(8), 17-25, 1999.
- [4] Prabhu K..N., Shivaprasada K., and Udupa K.R, Assessment of degree of modification in Al-Si eutectic alloy (LM6) by NDT techniques, *Indian Foundry Journal*, 45(9), 177-183, 1999.
- [5] Kori S.A., Murty B.S., and Chakraborty M, Grain refinement of Al-Si alloys, *Indian Foundry Journal*, 45(1), 7-19, 1999.
- [6] James R.H., Casting aluminium alloy casting process, *Modern Castings*, 9-16, 1965.
- [7] Vernaza Pena, K. M., Mason J. J. and Li M., High speed temperature measurements in orthogonal cutting of aluminum, *Experimental Mechanics*, 42, 221-229, 2003.
- [9] Trent. E. M., and Wright P. K., Metal cutting, Butterworth-Heinemann, Boston, fourth edition, 2000.
- [10] Chennakesava Reddy, A., A method to evaluate surface roughness of as-castings, *Indian Foundry Journal*, 42 (12), 28-30, 1996.
- [11] Ezugwu E. O., High speed machining of aero engine alloys, *Journal of the Brazilian Society of Mechanical Sciences & Engineering*, Vol.26, No.1, 2004, pp.1-1
- [12] Chennakesava Reddy, A., and Ramesh Kumar, P., Analysis of core characteristics in VACM process using response surface methodology, *Indian Foundry Journal*, 142-146, 1998
- [13] Ross P.J., Taguchi techniques for quality engineering, McGraw Hill International Edition, Second Edition, New York, 1996.

- [14] Taguchi, G., Introduction to quality engineering, Asian Productivity Organization, 1986.
- [15] Shaw, M. C., Metal Cutting Principles, Oxford University Press, Inc., New York, second edition, 2005.

S. Madhava Reddy

Associate Professor, Department of mechanical Engineering
MGIT, Gandipet, hyderabad-75
E-mail: smrmec@gmail.com

A. Chennakesava Reddy

Professor and Head, Department of mechanical Engineering
JNTU College of engineering, JNTUH, Hyderabad., A.P
E-mail: dr_acreddy@yahoo.com